Published in final edited form as:

Pigment Cell Melanoma Res. 2019 November ; 32(6): 753–765. doi:10.1111/pcmr.12791.

The TYRP1-mediated protection of human tyrosinase activity does not involve stable interactions of tyrosinase domains.

Monika B. Dolinska[1], **Paul T. Wingfield**[2], **Kenneth L. Young II**[1], **Yuri V. Sergeev**[1]

[1]National Eye Institute, National Institutes of Health, 31 Center Drive MSC 2510, Bethesda, MD 20892, USA

[2]National Institute of Arthritis and Musculoskeletal and Skin Diseases, National Institutes of Health, 31 Center Dr. - MSC 2350, Bethesda, MD 20892, USA

Summary

Tyrosinases are melanocyte-specific enzymes involved in melanin biosynthesis. Mutations in their genes cause oculocutaneous albinism associated with reduced or altered pigmentation of skin, hair, and eyes. Here, the recombinant human intra-melanosomal domains of tyrosinase, TYRtr (19 – 469), and tyrosinase-related protein 1, TYRP1tr (25 – 472), were studied *in vitro* to define their functional relationship. Proteins were expressed or coexpressed in whole *Trichoplusia ni* larvae and purified. Their associations were studied using gel filtration and sedimentation equilibrium methods. Protection of TYRtr was studied by measuring the kinetics of tyrosinase diphenol oxidase activity in the presence (1:1 and 1:20 molar ratios) or the absence of TYRP1tr for 10 hr under conditions mimicking melanosomal and ER pH values. Our data indicate that TYRtr incubation with excess TYRP1tr protects TYR, increasing its stability over time. However, this mechanism does not appear to involve the formation of stable hetero-oligomeric complexes to maintain the protective function.

Keywords

tyrosinase; tyrosinase-related protein 1; protein stability; protein purification; oculocutaneous albinism

Introduction

In general, pigments are responsible for colors in any organic or inorganic material. Melanin (from Greek *melanos*, meaning “dark, black”) is the main biological pigment found in mammals. Animals use the pigmentation for mimicry, camouflage, and communication or as a warning to predators. In humans, the determinants of skin, hair, and eye color are due to the varying ratio of two types of melanin: brown/black (eumelanin) and yellow/red (pheomelanin). Human melanin plays a crucial role in skin photoprotection from sunlight

Correspondence: Yuri Sergeev, Ophthalmic Genetics and Visual Function Branch, National Eye Institute, National Institutes of Health, 10 Center Dr., Bethesda, MD 20892, Tel: 301-594-7053/ Fax: 301-451-5758, sergeevy@nei.nih.gov.

Ethical Approval: This manuscript is not based on human/animal studies.

damage by absorbing and reflecting UV light (Pugliese, 1995, Virador et al., 1999). It is also a powerful antioxidant and free radical scavenger.

Melanin biosynthesis, also referred to as melanogenesis, is a complex process limited to melanosomes and is predominately regulated by melanogenic enzymes such as tyrosinase (TYR, EC 1.14.18.1), tyrosinase-related protein 1 (TYRP1, EC 1.14.18.-), and tyrosinase-related protein 2 (TYRP2/DCT, EC 5.3.3.12). These three enzymes are Type 1 membrane glycoproteins with ~40% sequence homology and structurally similar tyrosinase domains maintaining conserved binding sites that are essential for tyrosinase catalytic activity with Cu^{2+} or Zn^{2+} atoms (Olivares and Solano, 2009) (Figure S1). According to a current view (Figure 1), TYR catalyzes the rate-limiting hydroxylation of L-tyrosine to L- 3,4-dihydroxyphenylalanine (L-DOPA) and the oxidation of L-DOPA to dopaquinone, as well as the oxidation of 5,6-dihydroxyindole (DHI) to indole 5,6-quinone (IQ). TYRP1 catalyzes the oxidation of 5,6-dihydroxyindole-2-carboxylic acid (DHICA) into indole-5,6-quinone-2-carboxylic acid (IQCA), and TYRP2 is responsible for the conversion of L-dopachrome into DHICA. Recently, the crystal structure of truncated TYRP1 was determined at 2.3 Å resolution (Lai et al., 2017), but the atomic structure of human TYR is unknown. While crystals are available for many bacterial and fungal tyrosinase species, attempts at crystallography of truncated human TYR have been unsuccessful (Lai et al., 2016).

TYRP1 is the most abundant protein in melanosomes and its associated with melanocyte differentiation (Tai et al., 1983, Vijayasaradhi et al., 1990). It was shown *in vivo* that TYRP1 plays a role in the stabilization of TYR and might contribute to the regulation of melanin production (Kobayashi et al., 1998, Hearing et al., 1992). Hearing's group study showed that TYRP1 functions as a molecular chaperone for TYR in the endoplasmic reticulum (ER), which suggests that interactions of TYRP1 with TYR occur in the ER (Toyofuku et al., 2001). It also suggested that heterodimeric species of TYR and TYRP1 are present in melanosomes from murine melanocytes (Kobayashi and Hearing, 2007). However, the specific molecular mechanism of TYR/TYRP1 chaperoning was not clear from these studies.

In contrast to experiments in cell culture, experiments with purified proteins allow us to exclude the complexity of the cell environment and determine the individual protein interactions in a controllable fashion *in vitro*. Therefore, we model recombinant TYR and TYRP1 reactions in conditions that mimic the melanosome and ER environments. Indeed, mammalian organelles exhibit distinct acidity; the environment is neutral in the ER (7.2), mildly acidic in the Golgi (6.4), and acidic within the granules (~5.0) (Miesenbock et al., 1998, Wu et al., 2000). Melanosomes, as endosome/lysosome-related organelles, are expected to have a pH of approximately 5, which was confirmed experimentally by numerous studies (Puri et al., 2000, Fuller et al., 2001, Bellono et al., 2016a, Bellono et al., 2016b). Using fluorescein diacetate, it was shown that the internal pH of melanosomes is even lower, falling in the range 3.0–4.6 (Bhatnagar et al., 1993). This group also demonstrated that the pH of melanosomes is inversely correlated with the degree of melanization. Moreover, some studies illustrated that as melanosomes mature, their pH increases, while other studies, by contrast, showed melanosomes mature independently of changes in pH and remained acidic throughout maturation (Raposo et al., 2001, Saeki and

Oikawa, 1983, Devi et al., 1987, Puri et al., 2000). Interestingly, melanosomes derived from the light-skin donors are more acidic than those derived from dark-skin donors; however, tyrosinases from melanocytes derived from both donors have the same optimum activity (Fuller et al., 2001). These data indicate that TYR and TYRP1 can function at different pH values.

Previously, we purified and biochemically characterized the intra-melanosomal domain of human recombinant TYR (TYRtr, residues 19–469) (Dolinska et al., 2014). A C-terminal short transmembrane fragment was deleted to avoid potential protein insolubility while preserving all other functional features of the enzymes. We have shown that TYRtr is a soluble monomeric glycoprotein with a weight-average molecular weight of ~57 kDa, which exhibits both monophenolase and diphenol oxidase enzymatic activities. The monomeric form of tyrosinase was confirmed in different sources, including bacteria (McMahon et al., 2007), mushroom (Wichers et al., 1996) and fungus (Gutteridge and Robb, 1975); however, some monomers might associate in tetramers (van Gelder et al., 1997). Tyrosinase was homo-dimeric in fungi (Fujieda et al., 2013), squid (Naraoka et al., 2003) and mouse melanocytes (Francis et al., 2003).

Human tyrosinases obtained from larval expression, possess glycosylation binding sites, which are very similar to the positions from human species (Dolinska et al, 2014). The glycosylation of tyrosinase is important for protein stability (Dolinska and Sergeev, 2017). However, the chemical structure of glycans in human is still not known. Therefore, we cannot exclude the possibility that the glycans could change native protein-protein interactions in pre-Golgi conditions in human cells.

Recently, we suggested a direct link between conformational stability and enzymatic activity of tyrosinase intra-melanosomal domains (Dolinska et al., 2017). In addition, to check how the presence of the transmembrane helix at the C terminus is responsible for TYR oligomerization, we purified and characterized the Type 1 membrane protein TYR and showed that when solubilized in detergent micelles, TYR exists as a monomeric protein (Kus et al., 2018). Our preliminary *in vitro* results contradict the view that tyrosinases must oligomerize to perform their function in the cell. To resolve this disparity, we performed a deep association study of human tyrosinases.

Here, the intra-melanosomal domains of TYR and TYRP1 (TYRtr and TYRP1tr) were expressed or coexpressed in whole *Trichoplusia ni* (*T. ni*) larvae and purified. Their associations were tested using gel filtration (GF) and sedimentation equilibrium (SE) methods. The protection of TYRtr function was studied at different molar ratios using a standard chaperoning assay by measuring the kinetics of TYRtr diphenol oxidase activity in the presence (1:1 and 1:20 molar ratios) or absence of TYRP1tr under conditions mimicking melanosome (pH 5.5) and ER (pH 7.2) environments for 10 hr. In addition, we studied the potential hetero-association of TYR/TYRP1. Our data indicate that TYRtr incubation with excessive amounts of TYRP1tr protects TYRtr, increasing its stability over time. However, this mechanism does not appear to involve the formation of stable hetero-oligomeric complexes to maintain the protective function.

Methods

Expression of proteins

Recombinant full-length human TYR (residues 19–529) and TYRP1 (residues 25–537) and their intra-melanosomal domains, TYRtr (residues 19 – 469) and TYRP1tr (residues 25 – 472), were expressed separately as previously described (Dolinska et al., 2014, Dolinska et al., 2017, Kus et al., 2018). All proteins contained a 6x His-tag on their C terminus. In addition, four different combinations of the same proteins, TYRtr/TYRP1tr, TYR/TYRP1, TYRtr/TYRP1, and TYR/TYRP1tr, were prepared by coinfection with baculoviruses at a 1:1 ratio, and each combination of proteins was independently coexpressed in *Ti. ni* larvae (Figure 2D). DNA constructs, baculovirus preparation, and protein expression in whole larvae were performed commercially at Allotropic Tech, LLC (https://allotropictech.com/).

Purification of proteins

Globular protein domains.—The recombinant intra-melanosomal domains of TYR and TYRP1 and their mixtures were purified using methods previously described (Dolinska et al., 2014) with some modifications. Briefly, infected larvae overexpressing TYRtr or TYRP1tr and frozen at −80°C were homogenized in 5x (vol/weight) Lysate Buffer (20 mM sodium phosphate, pH 7.4, 500 mM NaCl, 5 mM imidazole, 25 μM 1-phenyl-2-thiourea (PTU, Sigma-Aldrich, MO), 2 mM $MgCl_2$, 40 μg/ml DNAse I (Thermo Fisher Scientific, PA), 0.2 mg/ml lysozyme, complete set of protease inhibitors (Roche, USA)). After 15 min of incubation on a rotator, lysates were sonicated for 10 min and centrifuged at 10,600 x *g* for 30 min at 4°C. Then, supernatants were diluted 1:1 (v/v) with binding buffer (20 mM sodium phosphate, pH 7.4, 500 mM NaCl, 5 mM imidazole) and purified by IMAC followed by GF chromatography using a ÄKTAxpress liquid chromatography system equipped with UNICORN 5.31 software (GE Healthcare, NJ). The crude lysates were automatically loaded on a 5 ml His-Trap Crude IMAC column (GE Healthcare, NJ) pre-equilibrated with binding buffer and eluted with a linear gradient of 0–500 mM imidazole at a flow rate of 1 ml/min into a 13 ml loop. Then, the proteins were applied to a Sephacryl S-300 HR 26/60 column (GE Healthcare, NJ) pre-equilibrated with GF buffer (50 mM Tris-HCl, pH 7.4, 1 mM EDTA, 150 mM NaCl, 50 μM tris(2-carboxyethyl)phosphine (TCEP)) and collected as 2 ml fractions on a 96 well plate. Fractions containing protein of interest were combined and concentrated using Amicon Ultra-15/10,000 NMWL centrifugal filter units (Millipore Sigma, MA).

Membrane proteins.—Full-length TYR and TYRP1 and their mixtures were purified in the presence of Fos-choline-12 (Anatrace, OH) by IMAC and GF chromatography using a Bio-Logic Duo-Flow Maximizer workstation (Bio-Rad, CA). Crude lysates were loaded on a 5 ml His-Trap FF Crude IMAC column pre-equilibrated with binding buffer containing Fos-choline-12 and then eluted with a linear gradient of 0–500 mM imidazole. Fractions containing the protein of interest were dialyzed overnight against four liters of GF buffer containing Fos-choline-12 and concentrated using Amicon Ultra 10,000 NMWL centrifugal filter units. Proteins were further purified by GF using Sephacryl S-300 HR 16/60 and 30 ml Superdex 200 Increase GL 10/300 columns (GE Healthcare, NJ).

Identification of proteins

GF columns were calibrated using the Bio-Rad GF standards thyroglobulin (670 kDa), γ-globulin (158 kDa), ovalbumin (44 kDa), and myoglobulin (17 kDa). The concentration of proteins after each step of purification was determined using $A_{280nm/260nm}$ determined using a NanoDrop 2000c UV-Vis spectrophotometer (Thermo Scientific, DE). Proteins were analyzed by SDS-PAGE using 4–15% polyacrylamide gels (Bio-Rad, CA) stained with Thermo Scientific GelCode Blue reagent (Thermo Scientific, IL). Protein identity was confirmed by Western blot analysis using anti-TYR (T311, 1:2000 dilution) and anti-TYRP1 (G17, 1:500 dilution) antibodies (Santa Cruz Biotechnology, CA). Protein purity in the extracts during purification was determined from the SDS-PAGE gels using UN-SCAN-IT gel ™ gel analysis software (Silk Scientific, Inc., UT).

Analysis of potential TYR and TYRP1 hetero-association

Potential TYR and TYRP1 hetero-association was analyzed in several different sets of experiments, as shown in Figure 2:

1. Pure TYRtr and TYRP1tr mixed in a 1:1 or 1:20 ratio and incubated at RT for 24 hr (Panel **A**).
2. Larva-expressed TYRtr and TYRP1tr individually mixed at a ratio of 1:1 and purified together as soluble proteins (see “Purification of proteins” section) (Panel **B**).
3. Larva-expressed TYR and TRP1 individually mixed at a ratio of 1:1 and purified together in the presence of Fos-choline-12 (Anatrace, OH) as described in the “Purification of proteins” section (Panel **C**).
4. Four mixtures of two proteins, TYRtr/TYRP1tr, TYR/TYRP1, TYRtr/TYRP1, and TYR/TYRP1tr, were obtained from larvae by equimolar coinfection and purified as described in the “Purification of proteins” section (Panel **D**).

Pure protein combinations were applied to a Superdex 200 Increase GL 10/300 column (GE Healthcare, NJ) and eluted from the column on a Bio-Logic Duo-Flow Maximizer workstation (Bio-Rad, CA) using GF buffer. The column was precalibrated with the GF standards (Bio-Rad, CA) thyroglobulin, γ-globulin, ovalbumin, myoglobin, and vitamin B12. The fractions containing the peaks were collected and concentrated using Amicon Ultra-15/10,000 NMWL centrifugal filter units (Millipore Sigma, MA). The protein concentration was determined using $A_{260/280\ nm}$ measured with a NanoDrop 2000c UV-Vis spectrophotometer (Thermo Scientific, DE). Protein identity was confirmed by Western blot analysis using anti-TYR (T311) and anti-TYRP1 (G17) antibodies (Santa Cruz Biotechnology, CA).

Copper and zinc content analysis

Metal content analysis was performed commercially using a standard protocol for inductively coupled plasma-mass spectrometry (ICP-MS) by Exova, CA. An entire sample (0.2 g) was mixed with internal standards and a solution of 0.1% ammonium hydroxide, 0.05% EDTA, and 0.05% Triton X-100, producing 2 g of solution for ICP-MS analysis.

Sedimentation equilibrium

Analytical ultracentrifugation was performed using a Beckman Optima XL-I analytical ultracentrifuge with absorption optics, an An-60 Ti rotor and standard double-sector centerpiece cells. Data were collected after 16–20 hr at 16,500 rpm and 20°C. Baselines were established by overspeeding at 45,000 rpm for 4 hr. Data were analyzed using the standard Optima XL-I Origin-based data analysis software. Protein partial specific volume was calculated from amino acid compositions (Cohn EJ, 1943). The carbohydrate content was assumed to be 10%, and using an average partial specific volume of 0.63 for N-linked carbohydrate (Shire, 1992), a partial specific volume of 0.711 g/mL was determined for TYRtr.

Tyrosinase enzymatic assay

The diphenol oxidase activities of TYRtr in the presence or absence of TYRP1tr were measured spectrophotometrically using L-DOPA (Sigma-Aldrich, MO) as a substrate (Lopez-Serrano et al., 2007, Jeong and Shim, 2004). TYRtr was incubated at 37°C with 1.5 mM L-DOPA in the absence or presence of TYRP1tr in proportional (1:1) and excess (1:20) quantities with each experiment independently repeated at pH 7.2 or pH 5.5. Activity was monitored for 10 hr by measuring the absorbance of the formed dopachrome at 475 nm ($\varepsilon_{dopachrome}$ =3700 M^{-1} cm^{-1}) each min using the SpectraMax i3 multimode detection platform (Molecular Devices, CA) and was analyzed by SoftMax Pro software, rev. 6.5.

The specific activity of TYRtr was determined as L-DOPA enzyme activity multiplied by the sample total volume and divided by total protein.

Kinetic parameters

The diphenol oxidase reaction rate (V) of TYRtr was determined in the presence or absence of TYRP1 using L-DOPA as a substrate at concentrations from 0.094 to 6 mM. All assays were performed at 37°C in 10 mM sodium phosphate buffer at pH 7.2 or 5.5. Absorbance was measured at 475 nm using the SpectraMax i3 multimode detection platform (Molecular Devices, CA). The Michaelis-Menten constant (K_m) and maximal velocity (V_{max}) of proteins were calculated from Michaelis-Menten plots. Michaelis-Menten curves were fitted with a corresponding nonlinear function using the OriginPro program (version 2018b, OriginLAB Corporation, MA).

Dynamic Light Scattering

Dynamic light scattering (DLS) experiments were performed using the Litesizer 500 (Anton Paar USA, VA). The proteins at 1 mg/ml were equilibrated at 25°C in 20 mM Tris buffer, pH 7.2 in the presence or absence of 10 mM $CaCl_2$. The intensity curve fittings and the hydrodynamic diameter were performed and calculated using the Kalliope 2.2.3 software (Anton Paar Kalliope Professional).

Molecular modeling

The structure of human tyrosinase was modeled as previously described (Kus et al., 2018). Briefly, the atomic structures for the tyrosinase intra-melanosomal domain and full-length

protein were modeled using the molecular visualization, modeling, and dynamic program YASARA (www.yasara.com). Crystal structures of human TYRP1tr (Lai et al., 2017), a tyrosinase from *Bacillus megaterium* (Sendovski et al., 2011), and the oxy-form of the copper-bound *Streptomyces castaneoglobisporus* tyrosinase complexed with a caddie protein (Matoba et al., 2006) were used as structural templates. The structure of the protein was incorporated into a phosphatidyl-ethanolamine lipid membrane, and the protein-membrane complex was optimized and equilibrated using 250 picoseconds of simulated annealing in water.

The structure of tyrosinase-related protein 1 was modeled using the crystal structure 5M8L from the RCSB database (http://www.rcsb.org/pdb/).

Results

Purification and characterization of tyrosinases

A summary of the protein characterizations performed in this study is shown in Table 1. TYRtr and TYRP1tr were expressed in whole insect *T. ni* larvae and purified as soluble proteins in milligram quantities by immobilized metal affinity (IMAC) and GF chromatography using a method previously described for TYRtr (Dolinska et al., 2017) (Figure S2 A). The presence of proteins during the purification steps was confirmed by SDS-PAGE and Western blot using an anti-TYR anti-TYRP1 antibody. Both methods showed heterogeneous, broad bands with polypeptide molecular masses of ~ 60 kDa, which were attributed to N-linked glycosylation. TYRP1tr total protein and its purity for each purification step are shown in Table S1.

Pure TYRtr and TYRP1tr were eluted from the Superdex 200 Increase 10/300 GL column as single monomeric peaks with an apparent molecular weight of 56.23 and 54.95 kDa, respectively (Figure S2 B). The monomeric conformation of TYRP1tr was confirmed by SE, which showed a protein weight-average molecular weight of 59.24 ± 2.25 kDa, assuming 10% carbohydrate mass due to protein glycosylation (Figure S2 C). The presence of Cu^{2+} or Zn^{2+} ions was tested in pure recombinant TYRtr and TYRP1tr using ICP-MS (Figure S1). According to the data, a sample of TYRP1tr contained both Cu^{2+} and Zn^{2+} ions, which were determined to have concentrations above the detection limits. In contrast, only Cu^{2+} was detected in TYRtr. The finding agrees with previous studies that reported tyrosinases from different sources containing copper ions (Cu^{2+}) in their active sites (Matoba et al., 2006, Zekiri et al., 2014, Kaintz et al., 2014, Solano, 2018). However, the metal cofactor in TYRP1 indicated that the protein sample has both metal ions. This result contradicts recent X-ray fluorescence data suggesting that the intra-melanosomal domain (residues 25–471) in crystallized human TYRP1 contains zinc ions (Zn^{2+}) only (Lai et al., 2017). The purified and characterized proteins were used in experiments on the potential protection of TYR by TYRP1 *in vitro*.

Diphenol oxidase activity of TYRtr is protected in the presence of TYRP1tr

TYR catalyzes the initial steps in the conversion of tyrosine to melanin through hydroxylation of L-tyrosine to L-DOPA (monophenolase activity) and oxidation of L-DOPA

to dopaquinone (diphenol oxidase activity) (Hearing, 1987, Olivares and Solano, 2009). Then, dopaquinone undergoes intramolecular cyclization to form cyclodopa, which is rapidly oxidized by a redox reaction with dopaquinone to give dopachrome (Ito and Wakamatsu, 2008) (Figure 1). Here, we studied the diphenol oxidase activity of TYRtr in the presence of TYRP1tr at ratios of 1:1 and 1:20. The activity was determined by monitoring the absorbance at a wavelength of 475 nm and measured for 10 hr at body and heat shock temperatures (37 and 43°C, respectively), each in conditions mimicking melanosomal and ER pH values (Figure 3). In general, all of the activity kinetic profiles from Figure 3A achieved a peak corresponding to a maximum dopachrome concentration, then concentration was low, and showed a spontaneous change due to scattering or no change at the end, possibly corresponding to different forms of pigment precipitation (Figure 3C). Therefore, the protective function of TYRP1tr was characterized by several parameters such as the initial velocity (V_o), maximum dopachrome concentration, period of maximum dopachrome formation, and period of precipitation. All these parameters were determined from the kinetic profiles, as schematically shown in Figure S3.

Figure 3B shows that V_0 and the maximum dopachrome concentration were low at pH 5.5, indicating that TYRtr may be partially inactivated due to instability at low pH. However, V_0 and dopachrome concentration proportionally increased with the TYRP1tr concentration. Moreover, extra time was required for dopachrome to reach its maximum concentration in the presence of TYRP1tr at both tested pH values; however, the delay was more significant at pH 5.5.

TYRtr diphenol oxidase activity induced the appearance of melanin-like precipitation (Figure 3 B, C). At pH 7.2, precipitation was observed at approximately 400 min. At pH 5.5, precipitation occurred 170 min earlier but was strongly delayed in the presence of TYRP1tr at a ratio of 1:1. Interestingly, at a ratio of 1:20, the precipitation did not occur or was minimal and started at approximately 500 min.

The specific activity of TYRtr was previously described (Dolinska et al., 2014, Dolinska et al., 2017). We have shown that the enzyme has its maximum activity near neutral pH. Here, we measured the specific activity of TYRtr in the presence of TYRP1tr at ratios of 1:1 and 1:20 at pH 7.2 and 5.5. The data are shown as a percentage of TYRtr diphenol oxidase activity measured at pH 7.2 (Figure 4A). At pH 5.5, the TYRtr specific activity was lower than that at pH 7.2, 41.67 ± 7.84%; however, in the presence of TYRP1tr at a ratio of 1:20, the activity increased to 68.17 ± 13.04%.

Kinetic parameters calculated for TYRtr diphenol oxidase activity showed that at both pH values, Michaelis-Menten constants (K_m) decreased ~50% in the presence of excess TYRP1tr (1:20 ratio), indicating that the L-DOPA binding affinity for the TYRtr active site is higher when TYRP1tr is abundant than when it is present at low concentrations (Figure 4 B, C; Table 2). From the V_{max} and K_m values, the enzyme turnover, k_{cat}, and enzyme efficiency, k_{cat}/K_m, were calculated, and they showed that TYRtr turnover in the presence of an excess of TYRP1tr was slightly low at pH 7.2 (~20%) and high at pH 5.5 (~25%). The TYRtr efficiency in the presence of excess TYRP1tr was ≈ 55% greater than the control

value at pH 7.2 and 200% greater at pH 5.5, suggesting that the tyrosinase efficiency increases with excess TYRP1.

TYR and TYRP1 do not form stable hetero-oligomers *in vitro*

Our *in vitro* data indicate that the intra-melanosomal domains of TYR and TYRP1 as well as the full-length membrane proteins do not form stable complexes together. We examined several different sets of experiments to verify interactions between those two proteins, as shown in Figure 2. The results of these experiments are briefly summarized in Table 1.

Pure TYRtr and TYRP1tr were mixed in 1:1 and 1:20 ratios and incubated at room temperature for 24 hr (Figure 2A). Both TYRtr/TYRP1tr mixtures were eluted from the Superdex 200 Increase 10/300 GL column as one single monomeric peak with an apparent molecular weight of 48.98 and 50.12 kDa for TYRtr/TYRP1tr ratios of 1:1 and 1:20, respectively. Leftward shifts of the elution peaks, toward higher molecular weights, were not observed. Moreover, both mixtures showed single bands on an SDS-PAGE gel with molecular masses of ~ 60 kDa that strongly reacted with anti-TYR and anti-TYRP1 antibodies (Figure 2A, **inset**). Monomeric conformations were confirmed in TYRtr/TYRP1tr mixtures by SE, which showed protein weight-average molecular masses of 59.17 = 2.62 and 57.48 = 2.40 kDa for the TYRtr/TYRP1tr ratios 1:1 and 1:20, respectively, assuming 10% mass from carbohydrates due to glycosylation of the protein (Figure 5). In brief, the results from the mixed pure proteins failed to show evidence of any stable hetero-oligomer formation between TYRtr and TYRP1tr.

Mixing the biomass of larvae individually expressing full-length or intra-melanosomal domains of TYR and TYRP1 was the basis of alternating experimental sets used to test potential TYR/TYRP1 hetero-association (Figure 2 B, C). Larvae were mixed in a ratio of 1:1 (TYRtr/TYRP1tr or TYR/TYRP1), and the proteins were purified by IMAC and GF chromatography.

The TYRtr/TYRP1tr larval mixture was purified using His-Trap FF Crude and Sephacryl S-300 HR 16/60 columns. From the S-300 column, which has an exclusion limit of ≈ 2000 kDa, three peaks eluted (Figure S4). We have previously reported that most of the active TYRtr eluted from the same column in Peak 3 (Dolinska et al., 2017). Here, we showed that some of both proteins TYRtr and TYRP1tr are present in the first two peaks with proteins in the mass range of 300–2000 kDa; however, in those fractions, proteins were highly aggregated. Most of the pure soluble proteins eluted in Peak 3. Likewise, most of the TYRtr and TYRP1tr from the larval mixture eluted in the same peak. When applied to a Superdex 200 Increase 10/300 GL column, they eluted as a single monomeric peak with an apparent molecular weight of 58.89 kDa (Figure 2B). In addition, the TYRtr/TYRP1tr larval mixture showed a single band on SDS-PAGE and Western blots with anti-TYR and anti-TYRP1 antibodies (Figure 2B, **inset**).

The TYR/TYRP1 larval mixture was purified using His-Trap FF Crude and Superdex 200 Increase 10/300 GL columns in the presence of Fos-choline-12 detergent (Figure S5). From the second, GF column, two peaks were eluted; however, TYR and TYRP1 were observed in only the first peak, with an apparent molecular weight of 93.33 kDa (Figure 2C). This result

was confirmed by SDS-PAGE and Western blots with anti-TYR and anti-TYRP1 antibodies (Figure 2C, **inset**). A leftward shift of the elution peak, toward higher molecular weights than the full-length TYR and TYRP1, was not observed. However, the increase in apparent mass can be attributed to membrane proteins eluting as a protein-detergent complex. Fos-choline-12 micelles show a molecular weight of ≈ 40 kDa, so the TYR/TYRP1 larval mixture consists of monomers if a 1:1 micelle-to-protein ratio is assumed.

In summary, the TYRtr/TYRP1tr or TYR/TYRP1 larval mixtures show no evidence of stable hetero-oligomer formation between TYR and TYRP1.

The last four experimental sets were based on the coexpression of full-length and intra-melanosomal domains of TYR and TYRP1 (Figure 2D). Four mixtures of two proteins, TYRtr/TYRP1tr, TYR/TYRP1, TYRtr/TYRP1, and TYR/TYRP1tr, were prepared by coinfection with baculoviruses at a 1:1 ratio, and each combination of proteins was independently coexpressed in larvae. Then, proteins were purified using IMAC and GF chromatography (Figure S6). All steps used to purify the coexpressed proteins from the larval biomass are shown in Table S2. Pure coexpressed proteins were eluted from a Superdex 200 Increase 10/300 GL column as single peaks with an apparent molecular weight of 63.10, 138.04, 117.49, and 134.90 kDa for the TYRtr/TYRP1tr, TYR/TYRP1, TYRtr/TYRP1, and TYR/TYRP1tr coexpressed proteins, respectively (Figure 2D). Fos-choline-12 was used for full-length protein purification. A leftward shift of the elution peaks, indicating an increase in the molecular weight, was observed for only the solutions including at least one membrane protein, which contained Fos-choline-12 detergent. This increase in apparent mass was attributed to membrane proteins eluting as a protein-detergent complex, assuming a 1:1 micelle-to-protein ratio. Moreover, the products showed single bands on SDS-PAGE and Western blots with anti-TYR and anti-TYRP1 antibodies (Figure 2D, **inset**); however, a strong smear was visible on the gel for coexpressed TYR/TRP1tr proteins. Weight-average molecular masses of 61.00 ± 2.62, 57.98 ± 2.60, 83.38 ± 4.12 and 61.21 ± 3.60 kDa for TYRtr/TYRP1tr, TYR/TYRP1, TYRtr/TYRP1, and TYR/TYRP1tr, respectively, obtained using SE, showed that the purified coexpressed tyrosinase/tyrosinase-related protein 1 proteins behave as separate monomeric glycoproteins or as if participating in a weak monomer-dimer equilibrium (Figure 5).

Discussion

Here, recombinant human TYRtr and TYRP1tr were expressed and coexpressed in whole *T. ni* larvae, and the proteins were then purified and characterized by GF and SE methods. To understand the functional role of TYRP1, the kinetics of tyrosinase diphenol oxidase activity were measured for an unusually long time (10 hr) in the presence (1:1 and 1:20 TYRtr/TYRP1tr molar ratios) or the absence of TYRP1tr under physiological or heat shock conditions in environments mimicking melanosomal and ER pH values. We demonstrated that at melanosomal pH values (pH 5.5), both tyrosinase catalytic activity and enzyme efficiency increase with excess TYRP1. Additionally, our experiments show that excess TYRP1tr protects tyrosinase function, as demonstrated by the increase in protein lifetime. The protective function of TYRP1 was demonstrated for the first time *in vitro*. This finding could be important for understanding the functions of tyrosinases in melanogenesis.

To determine the specific molecular mechanism underlying tyrosinase interactions, we analyzed the potential hetero-association between those two proteins using several different model systems in both *in vitro* and *in vivo* conditions. Using GF and SE methods, we illustrated that TYRP1tr is a monomeric glycoprotein with a weight-average molecular weight of ~60 kDa and does not form stable homo-dimers or higher homo-oligomers. Similar results were obtained previously for the intra-melanosomal domain of TYR (Dolinska et al., 2014).

Currently, direct experimental measurements of TYR/TYRP1 molar ratios in melanosomes are not available from the literature. However, there are several indirect indications that the concentration of TYRP1 molecules in melanosomes is significantly higher than the concentration of TYR molecules. Indeed, TYRP1 is the most abundant protein in melanosomes and its associated with melanocyte differentiation (Tai et al., 1983, Vijayasaradhi et al., 1990). It was shown *in vivo* that TYRP1 plays a role in the stabilization of TYR and might contribute to the regulation of melanin production (Kobayashi et al., 1998, Hearing et al., 1992). These data agree with our results suggesting a protective role of excess TYRP1 in the stabilization and improvement of tyrosinase function.

Previous studies *in vivo* suggested that TYRP1 functions as a molecular chaperone for TYR in the ER, which suggests that interactions of TYRP1 with TYR occur in the ER and that homo-oligomerization of TYR is a step in proper protein maturation within the ER (Toyofuku et al., 2001, Francis et al., 2003). In addition, heterodimeric species of TYR and TYRP1 were suggested to be present in melanosomes from murine melanocytes (Kobayashi and Hearing, 2007). However, the specific molecular mechanism of TYR/TYRP1 chaperoning and oligomerization was not clear from these studies. The idea that TYRP1 acts as a molecular chaperone was not confirmed in our *in vitro* experiments with recombinant tyrosinases. Indeed, there is no direct observation that TYRP1 helps tyrosinase maintain a native protein fold *in vitro*. Currently, the lectin chaperones calnexin and calreticulin, which are components of the ER quality control system, associate with TYR during protein folding (Petrescu, 2005). Second, there is no observation of TYRP1 consuming energy to perform the protective function, in contrast to chaperone-like molecules requiring ATP or GTP as an energy source to perform their function (Biswas and Das, 2004, Mendoza et al., 2012). Third, according to our data, TYRP1 is monomeric and does not form a large oligomeric homocomplex to provide a protein surface for the binding of misfolded proteins, as suggested previously (Glover and Clark, 2015, Jovcevski et al., 2015). From this view, the mechanism of the TYRP1 protection could be different from that of classical chaperone function.

Oligomeric proteins form through interactions of complementary surfaces of their subunits. The contact surface area should be at least ~500 $Å^2$ to form a stable protein complex. In chromatography, transiently interacting molecules with smaller and more ‘random’ associations will elute in positions different from that of protein complexes formed by stable interactions. Therefore, the excess of TYRP1 cannot hide stable oligomers in our experiments (ratios 1:1 or 1:20) *in vitro* using analytical grade GF and SE. Interestingly, however, we observed an improvement in catalytic activity and a 3-fold increase in TYRtr efficiency with a 20-fold excess of TYRP1tr at the pH of melanosomes (pH 5.5) (Figure 4A,

Table 2). The significant excess of TYRP1tr led us to the possible explanation that its protective effect could be related to molecular crowding, which is a mechanism that has been frequently reported for other proteins (Kuznetsova et al., 2014). Molecular crowding has been shown to enhance the protein stability, intrinsic catalytic efficiency, and structure of enterobactin-specific isochorismate synthase and the ATPase activity of the RNA-helicase eIF4A (Akabayov et al., 2013). The crowding effect is different from chaperoning (Minton, 2006). Crowding is characterized by molecular volume exclusion due to the excess of a highly concentrated protecting protein with decreases the available space ligands may occupy, bringing them in closer proximity to a corresponding active site (Minton, 2001), and complex pattern of interatomic interactions at protein surfaces (Sergeev et al., 2018). Therefore, molecular crowding might provide an explanation for the improvement in TYRtr function with excess of protecting protein, TYRP1tr. In addition, both molecular crowding and transient interactions between tyrosinase molecules might play a key role in melanosomal environments, where tyrosinase intra-melanosomal domains colocalized near the inner side of the melanosomal membrane with abundant quantities of TYRP1tr and high protein concentrations (Tai et al., 1983, Vijayasaradhi et al., 1990).

Certainly, our work demonstrated a very low propensity for the complex formation *in vitro*, with the definitive absence of stable association between two tyrosinases. This result suggests that in environments like those of melanosomes and the ER, TYR and TYRP1 do not form stable hetero-oligomeric complexes for maintaining protective function. However, this result could not exclude a role for transient interactions between two tyrosinases in the melanosomal environment. It is possible that these protein-protein interactions might be driven by weak electrostatic attraction provided by complementary electrostatic potentials, in contrast to the repulsive interactions in a neutral environment (Figure S7). Thus, the role of transient interactions could be critical for understanding the interactions of tyrosinases *in vivo*; it has previously been suggested that TYR forms a hetero-dimeric complex with TYRP1 (Kobayashi and Hearing, 2007).

It has been previously suggested that calcium is important for protein association in higher molecular weight forms (Orlow et al., 1994). In contrast, our experiments *in vitro*, performed in the absence and in the presence of calcium, confirmed the monomeric state of proteins using GF and DLS (Figure S8 A–C).

In addition, according to Orlow et al. protein purification and density centrifugation experiments were performed at 4°C. At this condition, tyrosinases could be affected by cold denaturation (Privalov, 1990), which could cause a change the protein native conformations (Shan et al., 2010). The change could be irreversible and could show higher-molecular-weight forms of non-active protein at certain condition (Hjorleifsson and Asgeirsson, 2016). Using pure proteins, we compared TYRtr activities at 3 different temperatures, 4, 25, and 37°C (Figure S8D). Pure TYRtr did show a very low protein activity at 4°C, suggesting cold denaturation. However, the active state of protein could be recovered *in vitro* at room temperature if protein is not damaged during the recovery. On other hand, it is also possible that some cell-specific effects were missed in our *in vitro* experiments. We also cannot exclude the possibility of TYRP2 having a critical role in oligomeric complex formation.

In conclusion, we have demonstrated *in vitro* that diphenol oxidase activity of TYRtr is protected in the presence of TYRP1tr. Surprisingly, an analysis of potential associations of the intra-melanosomal domains and full-length tyrosinases or their mixtures shows no stable hetero-associations between domains or whole molecules of the two recombinant, suggesting that another mechanism is the basis for the TYRP1-mediated protective function.

Supplementary Material

Refer to Web version on PubMed Central for supplementary material.

Acknowledgement:

This research was supported by the Intramural Research Program of the NIH, ZIA EY000476–10 to Y.V.S.

Abbreviations:

OCA1	oculocutaneous albinism Type 1 genetic disorder
OCA3	oculocutaneous albinism Type 3 genetic disorder
TYRtr	intra-melanosomal domain of human tyrosinase
TYRP1tr	intra-melanosomal domain of human tyrosinase-related protein 1
TYR	full-length membrane tyrosinase
TYRP1	full-length membrane tyrosinase-related protein 1
IMAC	immobilized metal affinity chromatography
GF	gel filtration (size-exclusion) chromatography
SE	sedimentation equilibrium
ICP-MS	inductively coupled plasma-mass spectrometry
L-DOPA	L-3,4-dihydroxyphenylalanine
PTU	1-phenyl-2-thiourea
DHI	5,6-dihydroxyindole
IQ	indole 5,6-quinone
DHICA	5,6-dihydroxyindole-2-carboxylic acid
IQCA	indole-5,6-quinone-2-carboxylic acid
CHO	carbohydrate

References

AKABAYOV SR, AKABAYOV B, RICHARDSON CC & WAGNER G 2013 Molecular crowding enhanced ATPase activity of the RNA helicase eIF4A correlates with compaction of its quaternary structure and association with eIF4G. J Am Chem Soc, 135, 10040–7. [PubMed: 23767688]

BELLONO NW, ESCOBAR IE & OANCEA E 2016a Corrigendum: A melanosomal two-pore sodium channel regulates pigmentation. Sci Rep, 6, 32274. [PubMed: 27573620]

BELLONO NW, ESCOBAR IE & OANCEA E 2016b A melanosomal two-pore sodium channel regulates pigmentation. Sci Rep, 6, 26570. [PubMed: 27231233]

BHATNAGAR V, ANJAIAH S, PURI N, DARSHANAM BN & RAMAIAH A 1993 pH of melanosomes of B 16 murine melanoma is acidic: its physiological importance in the regulation of melanin biosynthesis. Arch Biochem Biophys, 307, 183–92. [PubMed: 8239655]

BISWAS A & DAS KP 2004 Role of ATP on the interaction of alpha-crystallin with its substrates and its implications for the molecular chaperone function. J Biol Chem, 279, 42648–57. [PubMed: 15292216]

COHN EJ EJ 1943 Proteins, Amino Acids and Peptides. Princeton NJ: Van Nostrand-Reinhold, 48.

DEVI CC, TRIPATHI RK & RAMAIAH A 1987 pH-dependent interconvertible allosteric forms of murine melanoma tyrosinase. Physiological implications. Eur J Biochem, 166, 705–11. [PubMed: 3111852]

DOLINSKA MB, KOVALEVA E, BACKLUND P, WINGFIELD PT, BROOKS BP & SERGEEV YV 2014 Albinism-causing mutations in recombinant human tyrosinase alter intrinsic enzymatic activity. PloS one, 9, e84494. [PubMed: 24392141]

DOLINSKA MB, KUS NJ, FARNEY SK, WINGFIELD PT, BROOKS BP & SERGEEV YV 2017 Oculocutaneous albinism type 1: link between mutations, tyrosinase conformational stability, and enzymatic activity. Pigment cell & melanoma research, 30, 41–52. [PubMed: 27775880]

DOLINSKA MB & SERGEEV YV 2017 The consequences of deglycosylation of recombinant intra-melanosomal domain of human tyrosinase. Biol Chem, 399, 73–77. [PubMed: 28858842]

FRANCIS E, WANG N, PARAG H, HALABAN R & HEBERT DN 2003 Tyrosinase maturation and oligomerization in the endoplasmic reticulum require a melanocyte-specific factor. J Biol Chem, 278, 25607–17. [PubMed: 12724309]

FUJIEDA N, YABUTA S, IKEDA T, OYAMA T, MURAKI N, KURISU G & ITOH S 2013 Crystal structures of copper-depleted and copper-bound fungal pro-tyrosinase: insights into endogenous cysteine-dependent copper incorporation. J Biol Chem, 288, 22128–40. [PubMed: 23749993]

FULLER BB, SPAULDING DT & SMITH DR 2001 Regulation of the catalytic activity of preexisting tyrosinase in black and Caucasian human melanocyte cell cultures. Exp Cell Res, 262, 197–208. [PubMed: 11139343]

GLOVER DJ & CLARK DS 2015 Oligomeric assembly is required for chaperone activity of the filamentous gamma-prefoldin. FEBS J, 282, 2985–97. [PubMed: 26096656]

GUTTERIDGE S & ROBB D 1975 The catecholase activity of Neurospora tyrosinase. Eur J Biochem, 54, 107–16. [PubMed: 807476]

HEARING VJ JR. 1987 Mammalian monophenol monooxygenase (tyrosinase): purification, properties, and reactions catalyzed. Methods Enzymol, 142, 154–65. [PubMed: 3110555]

HEARING VJ, TSUKAMOTO K, URABE K, KAMEYAMA K, MONTAGUE PM & JACKSON IJ 1992 Functional properties of cloned melanogenic proteins. Pigment Cell Res, 5, 264–70. [PubMed: 1292007]

HJORLEIFSSON JG & ASGEIRSSON B 2016 Cold-active alkaline phosphatase is irreversibly transformed into an inactive dimer by low urea concentrations. Biochim Biophys Acta, 1864, 755–65. [PubMed: 27043172]

ITO S & WAKAMATSU K 2008 Chemistry of mixed melanogenesis--pivotal roles of dopaquinone. Photochem Photobiol, 84, 582–92. [PubMed: 18435614]

JEONG CH & SHIM KH 2004 Tyrosinase inhibitor isolated from the leaves of Zanthoxylum piperitum. Biosci Biotechnol Biochem, 68, 1984–7. [PubMed: 15388977]

JOVCEVSKI B, KELLY MA, ROTE AP, BERG T, GASTALL HY, BENESCH JL, AQUILINA JA & ECROYD H 2015 Phosphomimics destabilize Hsp27 oligomeric assemblies and enhance chaperone activity. Chem Biol, 22, 186–95. [PubMed: 25699602]

KAINTZ C, MAURACHER SG & ROMPEL A 2014 Type-3 copper proteins: recent advances on polyphenol oxidases. Adv Protein Chem Struct Biol, 97, 1–35. [PubMed: 25458353]

KOBAYASHI T & HEARING VJ 2007 Direct interaction of tyrosinase with Tyrp1 to form heterodimeric complexes in vivo. J Cell Sci, 120, 4261–8. [PubMed: 18042623]

KOBAYASHI T, IMOKAWA G, BENNETT DC & HEARING VJ 1998 Tyrosinase stabilization by Tyrp1 (the brown locus protein). J Biol Chem, 273, 31801–5. [PubMed: 9822646]

KUS NJ, DOLINSKA MB, YOUNG KL 2ND, DIMITRIADIS EK, WINGFIELD PT & SERGEEV YV 2018 Membrane-associated human tyrosinase is an enzymatically active monomeric glycoprotein. PLoS One, 13, e0198247. [PubMed: 29870551]

KUZNETSOVA IM, TUROVEROV KK & UVERSKY VN 2014 What macromolecular crowding can do to a protein. Int J Mol Sci, 15, 23090–140. [PubMed: 25514413]

LAI X, SOLER-LOPEZ M, WICHERS HJ & DIJKSTRA BW 2016 Large-scale recombinant expression and purification of human tyrosinase suitable for structural studies. PloS one, 11, e0161697. [PubMed: 27551823]

LAI X, WICHERS HJ, SOLER-LOPEZ M & DIJKSTRA BW 2017 Structure of Human Tyrosinase Related Protein 1 Reveals a Binuclear Zinc Active Site Important for Melanogenesis. Angew Chem Int Ed Engl, 56, 9812–9815. [PubMed: 28661582]

LOPEZ-SERRANO D, SOLANO F & SANCHEZ-AMAT A 2007 Involvement of a novel copper chaperone in tyrosinase activity and melanin synthesis in Marinomonas mediterranea. Microbiology, 153, 2241–9. [PubMed: 17600068]

MATOBA Y, KUMAGAI T, YAMAMOTO A, YOSHITSU H & SUGIYAMA M 2006 Crystallographic evidence that the dinuclear copper center of tyrosinase is flexible during catalysis. J Biol Chem, 281, 8981–90. [PubMed: 16436386]

MCMAHON AM, DOYLE EM, BROOKS S & O'CONNOR KE 2007 Biochemical characterisation of the coexisting tyrosinase and laccase in the soil bacterium Pseudomonas putida F6. Enzyme and Microbial Technology, 40, 1435–1441.

MENDOZA JA, CORREA MD & ZARDENETA G 2012 GTP binds to alpha-crystallin and causes a significant conformational change. Int J Biol Macromol, 50, 895–8. [PubMed: 22387076]

MIESENBOCK G, DE ANGELIS DA & ROTHMAN JE 1998 Visualizing secretion and synaptic transmission with pH-sensitive green fluorescent proteins. Nature, 394, 192–5. [PubMed: 9671304]

MINTON AP 2001 The influence of macromolecular crowding and macromolecular confinement on biochemical reactions in physiological media. J Biol Chem, 276, 10577–80. [PubMed: 11279227]

MINTON AP 2006 Macromolecular crowding. Curr Biol, 16, R269–71. [PubMed: 16631567]

NARAOKA T, UCHISAWA H, MORI H, MATSUE H, CHIBA S & KIMURA A 2003 Purification, characterization and molecular cloning of tyrosinase from the cephalopod mollusk, Illex argentinus. Eur J Biochem, 270, 4026–38. [PubMed: 14511385]

OLIVARES C & SOLANO F 2009 New insights into the active site structure and catalytic mechanism of tyrosinase and its related proteins. Pigment cell & melanoma research, 22, 750–760. [PubMed: 19735457]

ORLOW SJ, ZHOU BK, CHAKRABORTY AK, DRUCKER M, PIFKO-HIRST S & PAWELEK JM 1994 High-molecular-weight forms of tyrosinase and the tyrosinase-related proteins: evidence for a melanogenic complex. J Invest Dermatol, 103, 196–201. [PubMed: 8040609]

PETRESCU SM 2005 Do calnexin and calreticulin have a role in melanin formation? IUBMB Life, 57, 455–7. [PubMed: 16012055]

PRIVALOV PL 1990 Cold denaturation of proteins. Crit Rev Biochem Mol Biol, 25, 281–305. [PubMed: 2225910]

PUGLIESE PT 1995 The skin, free radicals, and oxidative stress. Dermatol Nurs, 7, 361–9; quiz 370–1. [PubMed: 8703607]

PURI N, GARDNER JM & BRILLIANT MH 2000 Aberrant pH of melanosomes in pink-eyed dilution (p) mutant melanocytes. J Invest Dermatol, 115, 607–13. [PubMed: 10998131]

RAPOSO G, TENZA D, MURPHY DM, BERSON JF & MARKS MS 2001 Distinct protein sorting and localization to premelanosomes, melanosomes, and lysosomes in pigmented melanocytic cells. J Cell Biol, 152, 809–24. [PubMed: 11266471]

SAEKI H & OIKAWA A 1983 Stimulation of tyrosinase activity of cultured melanoma cells by lysosomotropic agents. J Cell Physiol, 116, 93–7. [PubMed: 6406524]

SENDOVSKI M, KANTEEV M, BEN-YOSEF VS, ADIR N & FISHMAN A 2011 First structures of an active bacterial tyrosinase reveal copper plasticity. J Mol Biol, 405, 227–37. [PubMed: 21040728]

SERGEEV YV, DOLINSKA MB & HEJTMANCIK JF 2018 Apoferritin is maintaining the native conformation of citrate synthase in vitro. J Anal Pharm Res, 7, 680–684. [PubMed: 30766967]

SHAN B, MCCLENDON S, ROSPIGLIOSI C, ELIEZER D & RALEIGH DP 2010 The cold denatured state of the C-terminal domain of protein L9 is compact and contains both native and non-native structure. J Am Chem Soc, 132, 4669–77. [PubMed: 20225821]

SHIRE SJ 1992 Determination of the Molecular Weight of Glycoproteins by Analytical Ultracentrifugation Technical Note DS-837. Palo Alto, CA: Beckman.

SOLANO F 2014 Melanins: Skin Pigments and Much More—Types, Structural Models, Biological Functions, and Formation Routes. New Journal of Science, 2014.

SOLANO F 2018 On the Metal Cofactor in the Tyrosinase Family. Int J Mol Sci, 19.

SUGUMARAN M & BAREK H 2016 Critical Analysis of the Melanogenic Pathway in Insects and Higher Animals. Int J Mol Sci, 17.

TAI T, EISINGER M, OGATA S & LLOYD KO 1983 Glycoproteins as differentiation markers in human malignant melanoma and melanocytes. Cancer Res, 43, 2773–9. [PubMed: 6850592]

TOYOFUKU K, WADA I, VALENCIA JC, KUSHIMOTO T, FERRANS VJ & HEARING VJ 2001 Oculocutaneous albinism types 1 and 3 are ER retention diseases: mutation of tyrosinase or Tyrp1 can affect the processing of both mutant and wild-type proteins. The FASEB Journal, 15, 2149–2161. [PubMed: 11641241]

VAN GELDER CW, FLURKEY WH & WICHERS HJ 1997 Sequence and structural features of plant and fungal tyrosinases. Phytochemistry, 45, 1309–23. [PubMed: 9237394]

VIJAYASARADHI S, BOUCHARD B & HOUGHTON AN 1990 The melanoma antigen gp75 is the human homologue of the mouse b (brown) locus gene product. J Exp Med, 171, 1375–80. [PubMed: 2324688]

VIRADOR VM, KOBAYASHI N, MATSUNAGA J & HEARING VJ 1999 A standardized protocol for assessing regulators of pigmentation. Anal Biochem, 270, 207–19. [PubMed: 10334838]

WICHERS HJ, GERRITSEN YAM & CHAPELON CGJ 1996 Tyrosinase isoforms from the fruitbodies of Agaricus bisporus. Phytochemistry, 43, 333–337.

WU MM, LLOPIS J, ADAMS S, MCCAFFERY JM, KULOMAA MS, MACHEN TE, MOORE HP & TSIEN RY 2000 Organelle pH studies using targeted avidin and fluorescein-biotin. Chem Biol, 7, 197–209. [PubMed: 10712929]

ZEKIRI F, MOLITOR C, MAURACHER SG, MICHAEL C, MAYER RL, GERNER C & ROMPEL A 2014 Purification and characterization of tyrosinase from walnut leaves (Juglans regia). Phytochemistry, 101, 5–15. [PubMed: 24613318]

Significance

Genetic mutations in TYR and TYRP1 cause different forms of oculocutaneous albinism. Here, we demonstrate a lack of stable associations between these two recombinant proteins. This result contradicts the current view suggesting hetero-dimerization during melanosome maturation. In addition, for the first time, TYRP1 has been shown to protect tyrosinase function *in vitro*, which could be critical for tyrosinase function at early stages of melanogenesis.

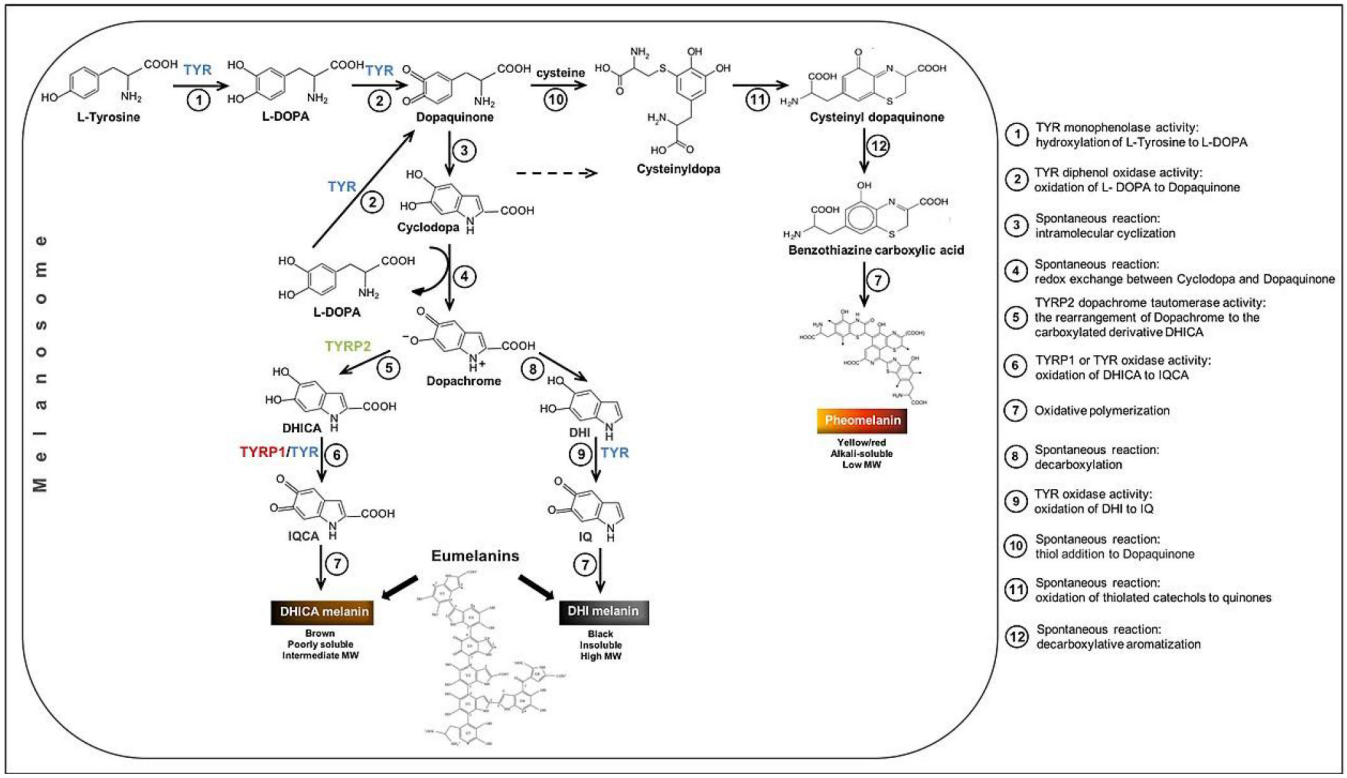

Figure 1. A current view of a melanogenic pathway leading to the production of melanins.

L-DOPA, L-3,4-dihydroxyphenylalanine; DHICA, 5,6-dihydroxyindole-2-carboxylic acid; IQCA, indole 5,6-quinone carboxylic acid; DHI, 5,6-dihydroxyindole; IQ, indole 5,6-quinone.

In the model of eumelanin structure, U1, U4, and U6 indolic units are DHI, but U2 and U5 are DHICA. Adapted from (Sugumaran and Barek, 2016, Solano, 2014, Ito and Wakamatsu, 2008).

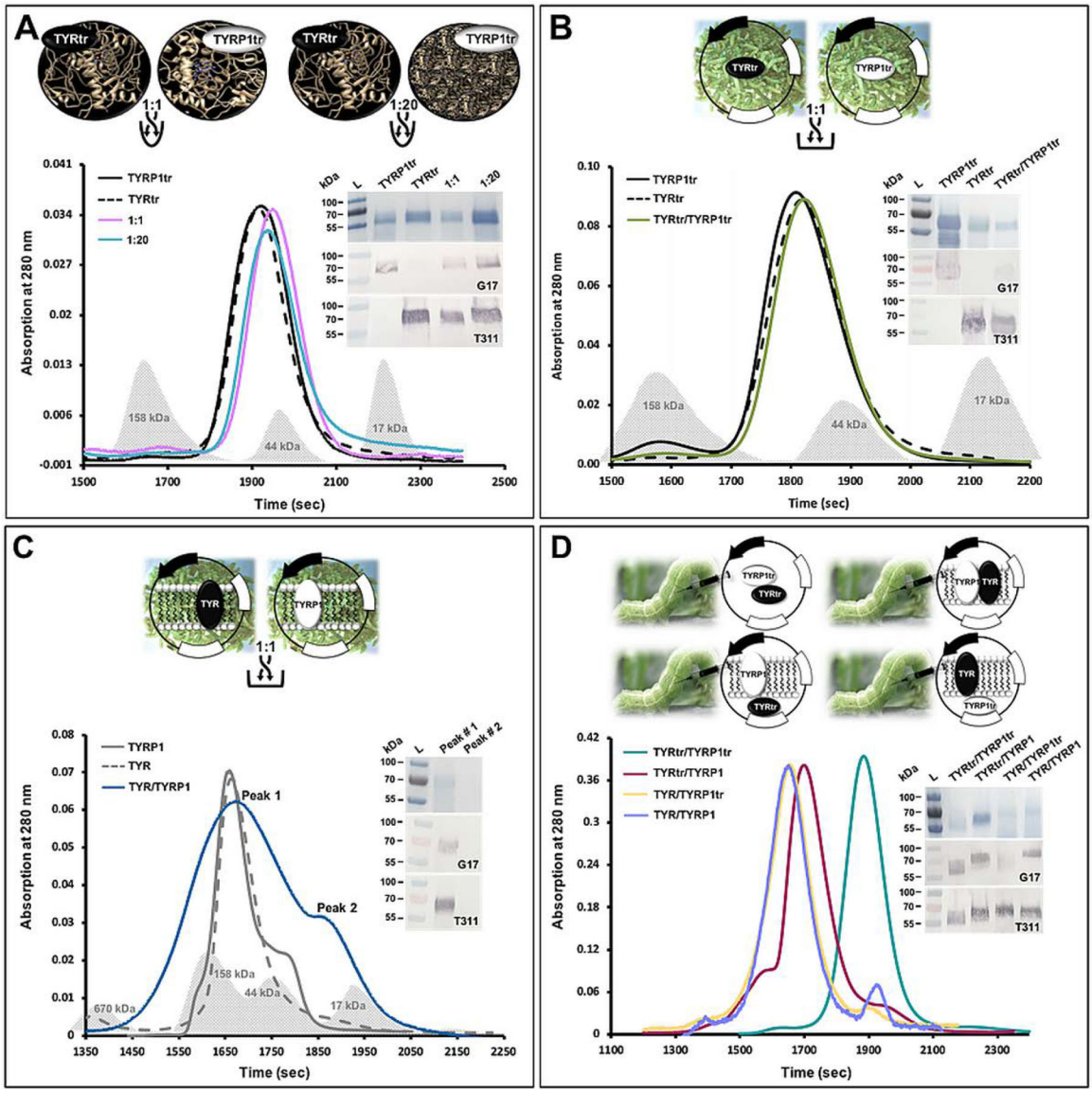

Figure 2. Experimental design for testing potential TYR/TYRP1 hetero-association.

Panel A: Individually purified TYRtr and TYRP1tr and their mixtures at 1:1 and 1:20 ratios. The graph shows the chromatography profiles of TYRtr (black dashed line), TYRP1tr (black solid lane), and TYRtr/TYRP1tr mixtures at a ratio of 1:1 (purple line) and 1:20 (cyan line). **Panel B:** Mixture of the intra-melanosomal domains of TYR and TYRP1 purified from the larval biomasses individually expressing both proteins. The graph shows the chromatography profiles of TYRtr (black dashed line), TYRP1tr (black solid lane), and a TYRtr/TYRP1tr biomass mixture at a ratio of 1:1 (green line). **Panel C:** Mixture of full-length TYR and TYRP1 purified from the larval biomasses individually expressing both proteins. The graph shows the chromatography profiles of TYR (gray dashed line), TYRP1 (gray solid lane), and a TYR/TYRP1 biomass mixture at a ratio of 1:1 (blue line), in which two peaks were observed. Gray shadows in each panel correspond to the Bio-Rad GF standards. **Panel D:** Four different combinations of proteins prepared by baculovirus

injection at a 1:1 ratio, independently coexpressed in *Ti. ni* larvae, and purified. The graph shows the chromatography profiles of TYRtr/TYRP1tr (green line), TYRtr/TYRP1 (red lane), TYR/TYRP1tr (yellow line), and TYR/TYRP1 (purple line).
The insets in each panel show the SDS-PAGE results (top panel) and Western blots using anti-TYRP1 (G17, middle panel) and anti-TYR antibodies (T311, bottom panel).

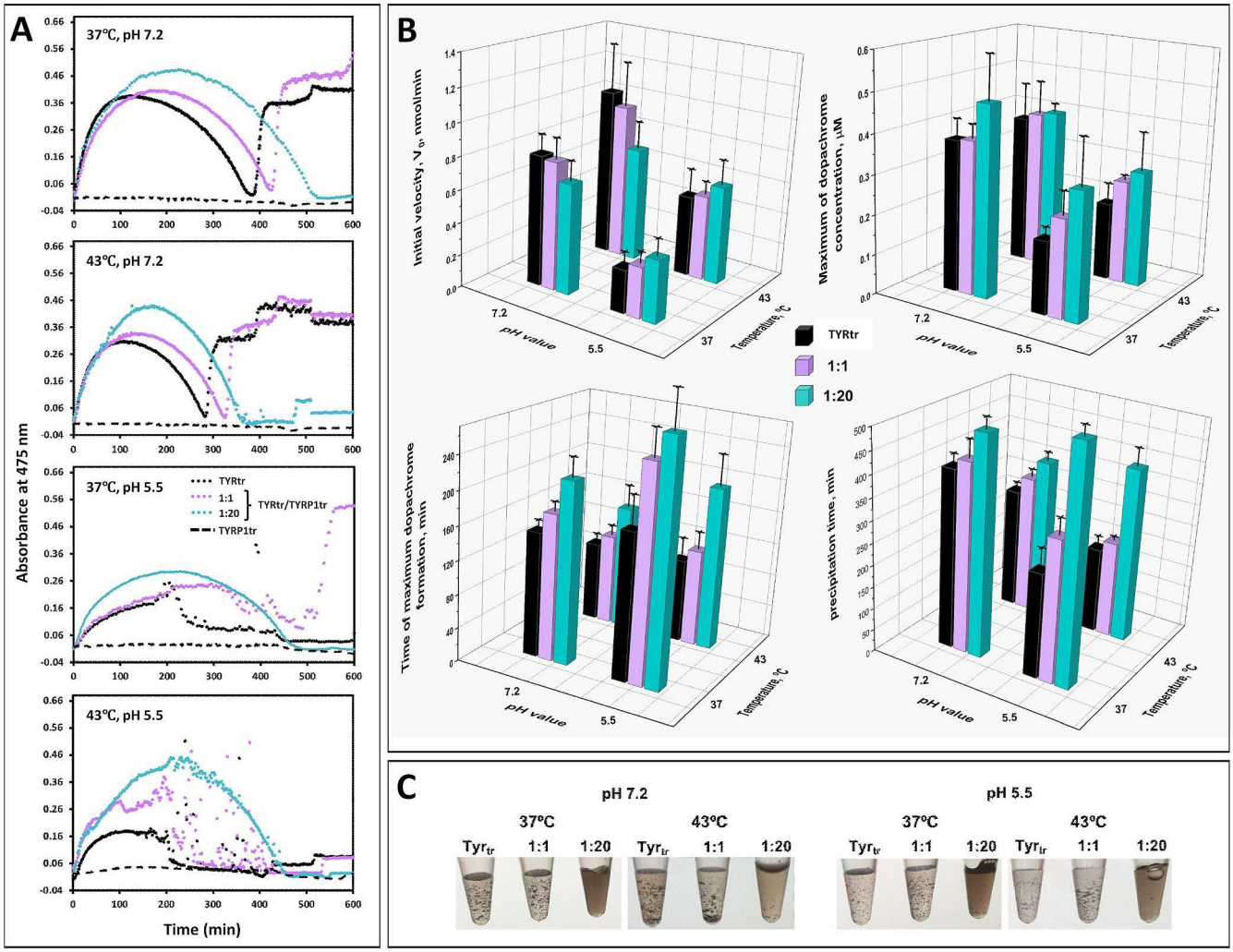

Figure 3. Dopachrome formation by TYRtr under TYRP1tr protection.

Panel A: Representative time curves of the diphenol oxidase activities of TYRtr alone (black dots) and in the presence of TYRP1tr in 1:1 (purple dots) and 1:20 (cyan dots) ratios at pH 7.2 and 5.5 and at temperatures of 37°C and 43°C. **Panel B:** The initial velocity (V_0), the initial linear rate of dopachrome formation, defined as the number of nmoles of dopachrome formed per minute, was calculated from the slope of the progress curve for a reaction (top left). Maximum of dopachrome concentration presented in μM using the Beer-Lambert law, A=εbc, where A is absorbance; ε is the extinction coefficient for dopachrome at 475 nm (3700 M^{-1} cm^{-1}); b is the path length of the well in which the sample is contained (cm); and c is the concentration of TYRtr in μM (top right). The time when the maximum dopachrome was formed is shown in minutes (bottom left). The melanin-like precipitation time is shown in minutes (bottom right). Values for TYRtr are shown as black bars, TYRtr in the presence of TRP1tr in a 1:1 ratio as purple bars, and TYRtr in the presence of TRP1tr in a 1:20 ratio as cyan bars. Errors represent the standard deviations from 3 independent experiments. **Panel C**: Pictures show melanin-like precipitation, which appeared during the incubation of L-DOPA with TYRtr and TYRtr/TYRP1tr mixtures in both 1:1 and 1:20 ratios at pH 7.2 and 5.5 and at temperatures of 37 and 43°C.

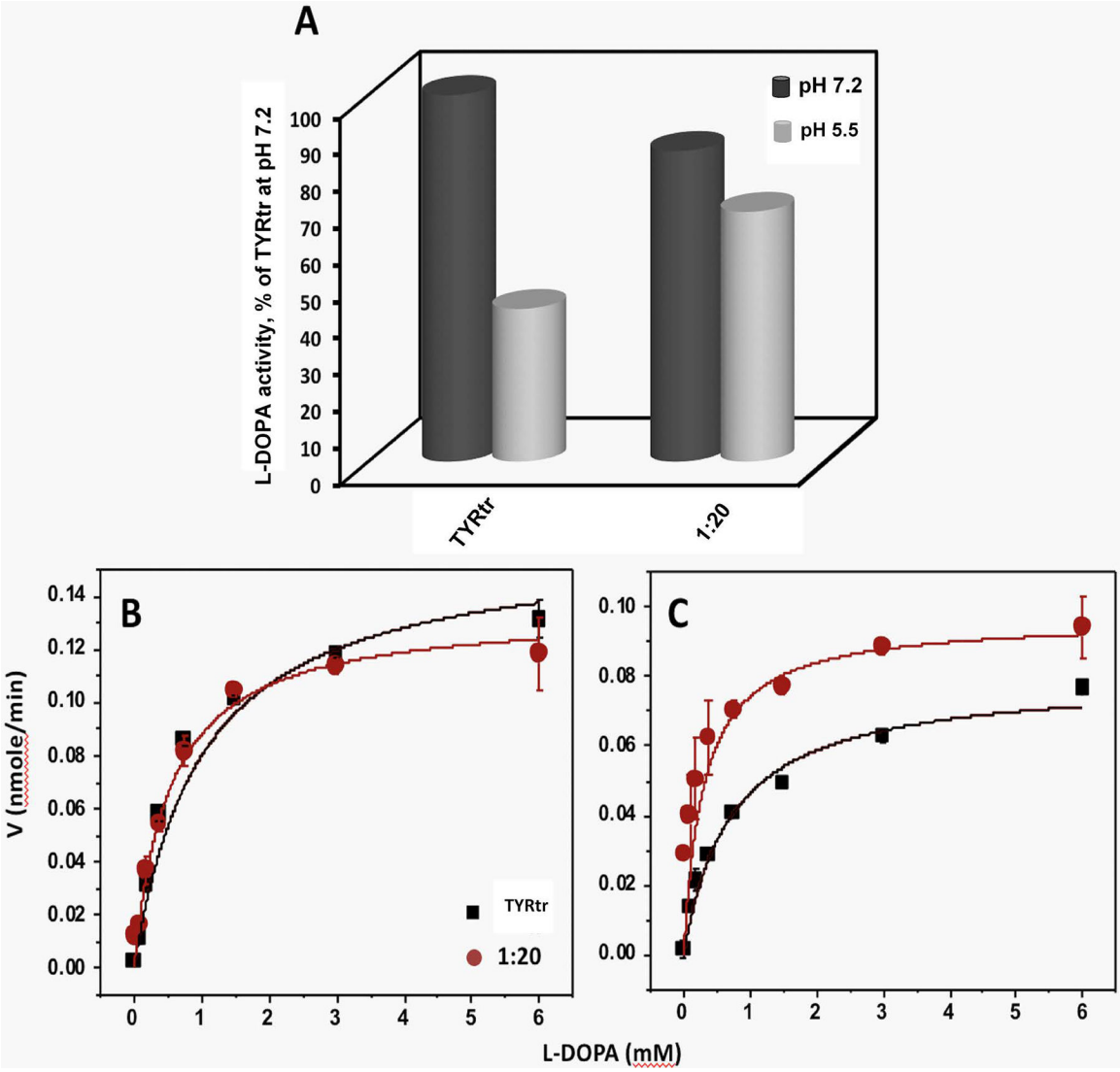

Figure 4. Enzymatic properties of TYRtr measured in the presence or absence of TYRP1tr.

Panel A: The specific activity of TYRtr in the presence or absence of an excess of TYRP1tr (1:20 ratio) was measured at pH 7.2 (black cylinders) and 5.5 (gray cylinders). All values are presented as a percentage of TYRtr activity measured at pH 7.2. **Panels B and C:** Michaelis-Menten plots of diphenol oxidase activities of TYRtr (black line) and TYRtr/TYRP1tr mixture in a 1:20 ratio (red line) as a function of L-DOPA concentrations measured at pH 7.2 (**Panel B)** and 5.5 **(Panel C)**. Enzyme assays were measured at 37°C. The lines represent nonlinear fits to the Michaelis-Menten equation. Experiments were performed in triplicate, and error bars represent standard deviations.

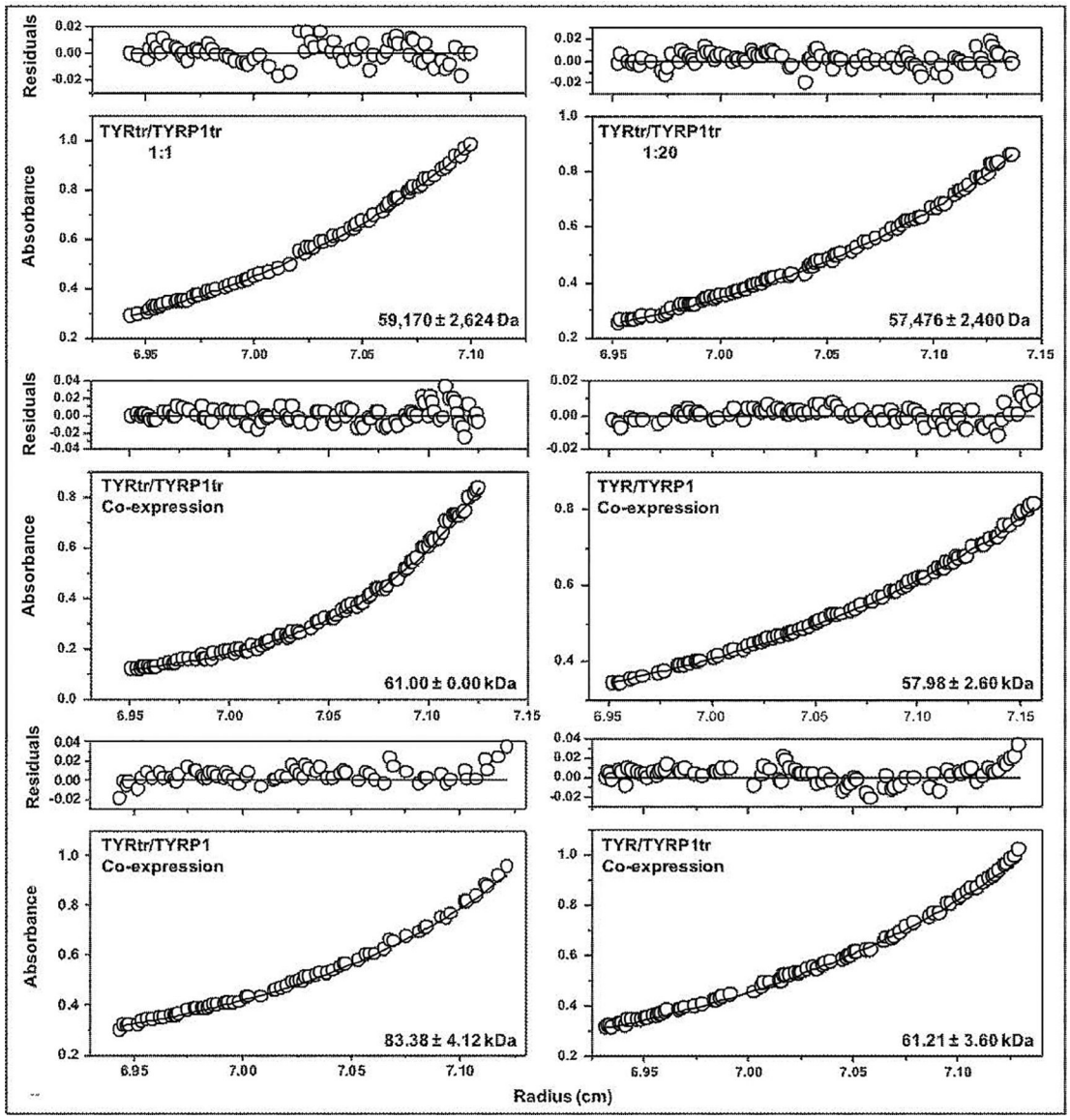

Figure 5.

Sedimentation equilibria of tyrosinases and their mixtures. Protein concentration profiles of absorbance (280 nm) versus radial distance are indicated. The black solid lines show the calculated fit for monomers. Open circles represent experimental values, but the open circles at the top show the residuals between fitted curves and data points.

Table 1.

Measurement of TYR and TYRP1 oligomeric state.

Protein or protein complex	Molecular weight (Da)				Oligomeric state
	sequence	10% CHO	GF	SE	
TYRtr	53,129	59,032	56,234	57,212[1]	monomer
TYRP1tr	54,305	60,339	54,954	59,240	monomer
TYR	61,216	68,018	141,254[2,4]	57,000[2]	monomer
TYRP1	61,547	68,386	105,000[3,4]	n/a	monomer
TYRtr/TYRP1tr (1:1)	107,434	119,371	48,978	59,170	Two monomers
TYRtr/TYRP1tr (1:20)	107,434	119,371	50,119	57,476	Two monomers
TYRtr/TYRP1tr biomass mixture	107,434	119,371	58,885	n/a	Two monomers
TYRtr/TYRP1tr biomass mixture	122,763	136,403	93,325	n/a	Two monomers
TYRtr/TYRP1tr coexpression	107,434	119,371	63,096	61,000	Two monomers
TYR/TYRP1 coexpression	122,763	136,403	138,038[4]	57,977	Two monomers
TYRtr/TYRP1 coexpression	114,676	127,418	117,490[4]	83,383	Two monomers or weak monomer-dimer equilibrium
TYR/TYRP1tr coexpression	115,521	128,357	134,896[4]	61,210	Two monomers

From left to right: sequence - molecular weight of polypeptide (Da); molecular weight of polypeptide assuming 10% carbohydrate content; apparent molecular weight estimated from GF; weight-average molecular masses obtained using SE. The sequences of human tyrosinase (EC 1.14.18.1) and tyrosinase-related protein 1 were obtained from the UniProtKB database (https://www.uniprot.org).

[1](Dolinska et al., 2014);

[2](Kus et al., 2018);

[3]unpublished data;

[4]protein in the Fos-choline-12 detergent.

Table 2.

Kinetic parameters of TYRtr measured in excess TYRP1tr.

	pH 7.2		pH 5.5	
	TYRtr	**1:20**	**TYRtr**	**1:20**
K_m (mM)	1.01 ± 0.18	0.53 ± 0.45	0.72 ± 0.11	0.30 ± 0.39
V_{max} (nmole/min)	0.16 ± 0.01	0.13 ± 0.02	0.08 ± 0.01	0.10 ± 0.02
k_{cat} (min^{-1})	3.20 ± 0.20	2.60 ± 0.40	1.60 ± 0.20	2.00 ± 0.40
k_{cat}/K_m (min^{-1}/mM)	3.17 ± 1.11	4.91 ± 0.87	2.22 ± 2.00	6.67 ± 1.03

K_m, Michaelis-Menten constant defining the affinity of L-DOPA for TYRtr, and V_{max}, the rate at which a L-DOPA is converted to dopachrome once bound to the TYRtr, were calculated from Michaelis-Menten plots fitted with the corresponding nonlinear function using OriginPro 2018b software; k_{cat} is the enzyme turnover, i.e., the number of L-DOPA molecules turned over per TYRtr molecule per minute, and was defined to equal V_{max}/E_t, where E_t is the TYRtr concentration (0.05 nM); k_{cat}/K_m, enzyme efficiency.